Study of Surface Wettability of Mineral Rock Particles by an Improved Washburn Method

Zheng Wang, Yanping Chu, Guozhong Zhao, Zhilin Yin, Tie Kuang, Feng Yan,* Lei Zhang, and Lu Zhang*

Read Online

ACCESS | Metrics & More | Article Recommendations

ABSTRACT: The surface wettability of rocks in underground reservoirs affects the distribution of fluids in the reservoir, so the wettability of reservoir minerals is a key factor for crude oil recovery from reservoirs. In this paper, the wettability of quartz sand with different particle sizes in different polar solvents was determined by Washburn's capillary rise method, and the $C·\cos\theta$ values were calculated first. Next, the experimentally obtained macroscopic contact angle of water on the quartz surface of 15.0° was substituted into $C·\cos\theta$ to obtain a linear equation between the particle size of quartz sand and the capillary constant C. The particle sizes of oil sand and mineral powder were then substituted into the equation to obtain their capillary constants C. Then, based on the Owens−Wendt−Rabel−Kaelbe (OWRK) equation and the obtained contact angles of solvent on quartz sand, oil sand, and mineral powder, the surface free energy of quartz sand with different particle sizes is calculated as 76.09, 76.65, and 76.42 mN/m, respectively, which are close to the literature results. In addition, the surface free energy of oil sand with different particle sizes was 23.22, 23.45, and 23.63 mN/m, and the results indicated that the polarity of oil sand was low. Meanwhile, the surface free energies of kaolinite, illite, feldspar, and montmorillonite were 61.59, 32.85, 35.87, and 25.91 mN/m, respectively. By the improved Washburn method in this paper, the wettability of different solvents on the surface of reservoir rocks was investigated, and the surface free energy of specific solid particles was calculated, which is important for studying the extraction of crude oil from subsurface reservoir rocks.
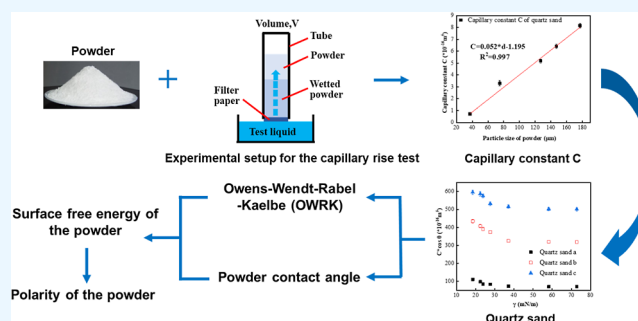
1. INTRODUCTION

Wettability is one of the most crucial elements in petroleum exploration and applications, and reservoir wettability has an impact on the distribution of reservoir fluid and oil recovery.[1] Due to the complex and variable structure of subsurface oil reservoirs and many irregular pores, a large number of clay minerals (such as montmorillonite, illite, and kaolinite) in oil-bearing reservoirs can be dispersed as fine particles distributed in the pores and form a surface coating in the pore space, which affects the surface wettability and oil recovery efficiency.[2]

For the determination of the surface wettability of solid particles, a porous media model is mainly considered.[3] The main methods are the sessile drop method, the Wilhelmy plate method, the liquid penetration method, and the Washburn capillary rise (WCR) method.[4] For the sessile drop method, although the pores between the powder particles also allow the liquid to penetrate, the contact angle measurement becomes difficult when the liquid penetrates faster.[5] By analyzing the Williams plate method, Dove et al.[6] found that when using a binder to apply the powder to the plate, it is difficult for the

powder to completely cover the surface of the plate.[7] Susana et al.[8] investigated through their study that the liquid permeation behavior is quite complex and highly dependent on the structure of the powder bed. Based on Washburn's equation and the capillary rise principle, the WCR method involves filling the sample tube with powder to allow spontaneous wetting to occur when the solution touches the bottom. Most of the powder filling methods use compact filling, which leads to consistent sample filling and reduces the possibility of powder collapse during the experiment.[9]

Several experimental and theoretical works have been carried out for the study of rock wettability in oil reservoirs. For example, Pan et al.[10] found that polar components adsorbed on the surface of clay minerals are easily aggregated and that crude

oil preferentially interacts with clay minerals in the pores. The experimental results of Rezaei Gomari and Joseph[11] showed that the crude oil and clay particle interaction leads to the adsorption of polar components of crude oil, which resulted in the change of the wettability of the sandstone surface to an oil-wet state. Robin et al.[12] proposed the importance of the geometry and mineral composition of porous media in determining the macroscopic wettability of rocks. Mamonov et al.[13] established a crude oil−brine−rock system and found that after exposure to crude oil of rocks, the water wettability of their surfaces decreased, which is mainly related to polar organic components. Therefore, the determination of surface wettability of clay mineral particles is extremely important for the study of surface wettability of rocks in subsurface oil reservoirs.

In recent years, there have been some studies on the WCR method for the determination of surface wettability of clay mineral particles. Klimenko et al.[14] found that the presence of crude oil compounds in the brine after contact with crude oil may influence the surface wettability of reservoir rocks. Kong et al.[15] studied the effect of powder size (48, 37, and 25 μm) on the surface wettability of clay minerals and found that the powder contact angle decreased significantly with decreasing mineral powder diameter for the same solvent. Fu et al.[17] investigated the wettability of organic solvents on montmorillonite by the Washburn method after mixing 63 μm montmorillonite with surfactants and found that surfactants affect the wettability of an organic clay surface.[16] Yang and Chang[18] proposed the lipophilic to hydrophilic ratio (LHR) concept based on Washburn's method, which was used to compare the selectivity of anthracite, manganese ore, and quartz sand to cyclohexane and water. The obtained LHR values were 1.93, 0.75, and 0.69, respectively, and it was found that anthracite is lipophilic, while manganese ore and quartz sand are hydrophilic. On this basis, Chang et al.[19] determined the LHR values of 66.87, 1.24, 1.22, 1.16, and 0.80 for the nutshell, manganese sand, ceramic particles, quartz sand, and ceramic sand, respectively. The results indicated that the nutshell was more lipophilic, while the ceramic sand was highly hydrophilic. Zhang and Luo[20] proposed a method based on the Good van Oss Chaudhury (GvOC) model to establish a system of equations to calculate the surface free energy of mineral powder. The obtained results were compared with those calculated by two other reference methods, and the differences were found to be within 5%.

In addition, oil sand particles contain fewer mineral components, and asphaltenes may be adsorbed on the surface of the oil sand, making the surface wettability of the oil sand exhibit hydrophobicity. Wang et al.[21] used a thin-film flotation method to determine the wettability of solids separated from oil sand and found that the thin-film flotation method could determine the inhomogeneity of solid particles based on the measured standard deviation. Chen et al.[22] found that organic solvents were surfactants, and asphaltenes on the surface of oil sand particles were highly soluble, and the washed oil sand particles exhibited some hydrophilicity. Dang-Vu et al.[23] found that the water droplet penetration method was the most sensitive in determining the wettability of solids extracted from oil sand compared to other methods. Liu et al.[24] measured the wettability of oil sand particles by the Washburn method and obtained a water contact angle of 88.8 ± 0.9°. Zelenev and Grenoble[25] found that water could wet the bitumen sand at a lower rate due to the presence of a small number of hydrophilic quartz particles in the bitumen sand.

The wettability of the reservoir surface is one of the key research fields in enhanced oil recovery, and the surface free energy of minerals is one of the key parameters. At present, there is no effective method to measure or calculate the surface free energy of oil sands. Therefore, a series of research works on such a difficult subject cannot be completed in a short time. The purpose of this paper is to investigate the wetting behavior of solid particles with different hydrophobicities in organic solvents and to determine the surface free energy of solid particles with different polarities. We substituted the macroscopic contact angle of water on the quartz surface of 15.0° obtained experimentally into $C \cdot \cos \theta$ to obtain a linear equation between the particle size of quartz sand and the capillary constant C. Then, we substituted the particle sizes of oil sand and mineral powder into the equation to obtain their capillary constants C. In this work, the powder contact angles of seven organic solvents on the surfaces of three solid particles were determined by the WCR method, and the experimental results were substituted into the OWRK equation to calculate the surface free energy of solid particles. It was found that the wetting behavior of the solvents on the surface of solid particles was greatly related to the surface tension of the solvents and the surface hydrophobicity of the solid particles.

2. MATERIALS AND METHODS

2.1. Materials. Deionized water (prepared by an ion exchange unit), formamide (99% purity), DMF (99% purity), ethanol (99% purity), cyclohexane (99% purity), *n*-decane (99% purity), *n*-hexane (99% purity), all solvents except deionized water were provided by Aladdin. Viscosity was measured with an Ubbelohde viscometer (Schott Instruments). The physicochemical properties of the liquids are shown in Table 1.

Table 1. Surface Free Energy of Various Solvents at 20 °C and Their Physicochemical Properties, Taken from the Literature[a][19,20,26−28]

solvent	density (g·cm^{-3})	viscosity (mPa·s)	surface tension (mN/m)		
			γ_l	γ_l^d	γ_l^p
deionized water	0.998	1.002	72.8	29.1	43.7
formamide	2.926	1.133	58.2	35.1	23.1
N,N-dimethylformamide (DMF)	0.941	0.850	37.1	29.0	8.1
ethanol	0.786	1.074	22.4	18.8	3.6
cyclohexane	0.774	0.998	28.1	26.5	1.6
n-decane	0.730	0.928	23.8	23.8	0
n-hexane	0.660	0.330	18.3	18.3	0

[a]Surface tension values measured by the Wilhelmy plate method.

Quartz sand provided by XinDe Mineral Material Ltd. (Gongyi, People's Republic of China) with particle sizes of 37 (a), 75 (b), 125 (c), 147 (d), and 177 μm (e), respectively. Oil sand particles provided by Daqing Oilfield Ltd. (Daqing, People's Republic of China) have particle sizes of 147 (a), 177 (b), and 250 μm (c). The mineral powder (kaolinite, illite, feldspar, and montmorillonite) with the particle size of 44 μm was provided by DeHang Mineral Products Ltd. (Shijiazhuang, People's Republic of China). Powder samples are sieved in a

vibrating sieve (GLS1020, Germany) to obtain powder particles of the corresponding particle size (37−250 μm). The diameter of the sieve holes (or mesh of the screen) is the particle size of the powder; therefore, the particle size of each powder particle is determined by the size of the sieve holes, and the particle size here refers to the diameter. In addition, it must be noted that the particle size here is an average value due to the dispersion of the powder particles.

2.2. Methods. *2.2.1. Washburn Capillary Rise.* The experimental instrument is the LAUDA Scientific GmbH instrument (Germany), and the experiments were conducted by the Washburn mass method to investigate the wettability of solid particles. The cleaned sample tube was dried and loaded into the measuring cell, then a filter paper sheet was placed above the outlet of the sample tube, and the measuring cell was fixed with a fixing nut.[20] Weigh a certain mass of powder particles into a glass tube (high 70 mm, inner diameter 7 mm), remove the funnel, and then load the powder sample in the sample tube according to the specific situation. The sample loading process was repeated several times for each experiment, and the average value was taken. In the process of filling the bed of powder, each experiment was repeated three times, and the average value was taken. It is critical to remember that the process of loading the powder is the most crucial step in the preparation of the entire experiment. Therefore, after the powder is filled, the mass of 500 g weights hanging on the push rod press the powder, and the height of each impact is maintained as closely as possible.[29] After several impacts, the height of the powder bed no longer changes, and then the powder loading process is completed. The purpose of this is to ensure the repeatability of the loading sample density and uniformity because it is directly related to the stability of the measurement results. The sample cell is placed on the measurement table, and the inlet pump unit is operated to add the analytical liquid to the measurement cell at an inlet rate of 300 μL/s until the liquid level of the indicator tube is parallel to the bottom of the sample tube. The experimental data is recorded when the bottom of the powder is just in contact with the liquid, and the experiment is completed when the liquid reaches the top of the powder particles or completely wets the powder. It is particularly important to note that in the process of filling the powder bed, each experiment is repeated three times, and the average value is taken.

Based on the Washburn equation and the capillary rise principle, the powder filling method used in the WCR method is compact filling. Such a filling method can avoid the measurement error caused by the liquid penetration into the powder particles between the pores in the fixed droplet method. The WCR method does not use a binder and therefore avoids the effect of the binder on the experiment. In addition, since the liquid permeation method exposes the solution directly to air during the experiment, the solution may volatilize and cause the contact angle of the powder to deviate from the actual contact angle; in the WCR method, the solution is inside the indicator tube (inner diameter: 2 mm) and the sample tube (inner diameter: 7 mm), which greatly reduces the experimental error caused by the volatilization of the solution compared with the liquid permeation method. Therefore, the WCR method was used in this paper to determine the powder wettability and calculate the powder contact angle.

WCR method assumes that powder or porous materials can be described as capillary bundles with a constant radius.[30] It is

derived from the principle of Poiseuille's law, defined as the existence of a linear relationship between the squared mass m^2 and the measurement time t.

$$m^2 = \frac{C\rho^2\gamma_{LV} \cos\theta}{\eta} t \tag{1}$$

$$C = rA^2\varepsilon^3 \tag{2}$$

Here, m is the mass of the permeating liquid (g), t is the rise time of the liquid permeation (s), ρ is the density of the liquid (g·cm^{-3}), γ_{LV} is the surface tension of the liquid (mN/m), η is the viscosity of the liquid (mPa·s), C is the capillary constant of the powder bed ($\times 10^{-16}$ m^5) (C depends on the "geometry" of the powder bed), r is the effective pore radius of the powder bed (cm), A is the cross-sectional area of the sample tube (cm^2), and ε is the void fraction of the powder material. The above equation can also be reduced to the square of the solution volume V^2 versus the capillary rise time t.

$$V^2 = \frac{C\gamma_{LV} \cos\theta}{\eta} t \tag{3}$$

In eq 3, V is the volume of the absorbing solution of the sample at a given time (μL). And in the Washburn equation above, V^2/t can be determined from the slope of the wetting curve. For known liquid properties (ρ, γ, and η), hence there are only two unknowns in the equation, C and θ. Transforming the above equation into the following form.

$$C \cdot \cos\theta = k\frac{\eta}{\gamma_{LV}} \tag{4}$$

In eq 4, k represents the wetting slope V^2/t (μL/s). The experimentally measured k is multiplied by the viscosity η of the solution of the wetted powder and then divided by the surface tension γ_{LV} to obtain the result of multiplying the capillary coefficient C with $\cos\theta$.

2.2.2. OWRK Method. The Washburn method was proposed mainly because the surface free energy of powder is difficult to measure directly due to the immobility of molecules in the solid phase. Many methods have been developed to estimate the surface free energy of a powder, such as measuring the contact angle of liquids by compressing the powder on a disk,[28] reverse air chromatography,[31] adsorption air chromatography,[32] and Washburn's dynamic contact angle measurement.[20] Among them, for the penetration of liquids into porous solid layers, the combination of the capillary rise method and Washburn's equation is the most widely used method, which is relatively simple and generally applicable. From the Washburn method, the contact angle θ can be obtained by calculation based on the slope of the obtained wetting curve of the powder when the surface tension and viscosity of the solvent are known. The surface tension components were proposed by Fowkes et al.,[33] who suggested that surface tension can be expressed as the sum of a series of surface tension components, each attributed to a specific type of intermolecular force. And these surface tension components were classified into two main types: dispersed and non-dispersed as Fowkes equation

$$\gamma_{sv} = \gamma_{sv}^p + \gamma_{sv}^d \tag{5}$$

where γ_{sv}^p is the polar surface free energy component of the solid and γ_{sv}^d is the nonpolar surface free energy component of the same solid. Owens and Wendt[34] proposed that the interfacial tension per phase can be divided into a polar

component γ^p and a non-polar component (dispersion component) γ^d. The OWRK approach can be used to express the relationship between the interfacial free energy γ_{sl} and the polar and nonpolar components of the solid−liquid surface free energy as follows

$$\gamma_{sl} = \gamma_{lv} + \gamma_{sv} - 2(\gamma_{lv}^d \gamma_{sv}^d)^{1/2} - 2(\gamma_{lv}^p \gamma_{sv}^p)^{1/2} \qquad (6)$$

In eq 6, γ_{sv}^d and γ_{lv}^d are the nonpolar components of the surface free energy of the solid and the liquid, respectively; γ_{sv}^p and γ_{lv}^p are the polar components of the surface free energy of the solid and the liquid, respectively. Young's equation, which describes the mechanical equilibrium of a liquid droplet in contact with a solid under the influence of three interfacial pressures, is frequently used to compute the surface free energy of solids.

$$\gamma_{sv} - \gamma_{sl} = \gamma_{lv} \cos\theta \qquad (7)$$

In eq 7, γ_{lv}, γ_{sv}, and γ_{sl} are the surface free energy of the liquid when the saturated vapor of the liquid becomes equilibrium, respectively, and the surface free energy of the solid and the interfacial free energy between the solid and the liquid. Combined eqs 7 and 6, which can get eq 8

$$\frac{\gamma_l(1 + \cos\theta)}{2\sqrt{(\gamma_l^d)}} = (\gamma_s^d)^{1/2} + (\gamma_s^p)^{1/2} \sqrt{\frac{\gamma_l^p}{\gamma_l^d}} \qquad (8)$$

By substituting the surface free energy γ_{lv}, the polar component γ_l^p and the non-polar component γ_l^d into eq 8, the $\gamma_{lv}(1 + \cos\theta)/2(\gamma_{lv}^d)^{1/2}$ graph of $(\gamma_{lv}^p/\gamma_{lv}^d)^{1/2}$ is obtained. The slope of the resulting line can be calculated from the polar component of the solid surface free energy γ_s^p, while the intercept of the line can be calculated from the non-polar component of the solid surface free energy γ_s^d, and the two are added to obtain the surface free energy γ_s of the solid.

2.2.3. Surface Tension and Contact Angle Measurements. The surface tension of the solvents was measured by a surface tension meter (Data Physics, Germany, DCAT21). Contact angle measurement by the fixed drop method using a LAUDA Scientific GmbH instrument (Germany). Acetone and ultra-pure water were used to ultrasonically clean the quartz plates for 30 min. Then, the quartz plates were immersed in the chromic acid solution for more than 6 h. The measurement was repeated five times by depositing droplets (2 μL) on the quartz plates. And the results were averaged five times, and the standard deviation of the contact angle values was less than 3°. Additional details of the contact angle measurements are in our previous work.[35]

3. RESULTS AND DISCUSSION

3.1. Typical Capillary Rise Curves. The wetting curves of quartz sand c and oil sand a particles in pure water and *n*-hexane are shown in Figure 1, and all experimental results are averaged over five repeatable experiments, as well as the variation of the volume squared of the solvent with increasing time. The good linearity of the wetting curves for each powder illustrates the suitability of Washburn's capillary rise method for determining the wettability of the particles. The slope of the wetting curve (V^2/t) of water for quartz sand is 35,220 μL^2/s and that of water for oil sand particles is 891 μL^2/s. The slope of the wetting curve (V^2/t) of quartz sand in *n*-hexane is 36,456 μL^2/s and that of *n*-hexane for oil sand particles is 12,969 μL^2/s. It can be found that the wetting slopes of *n*-
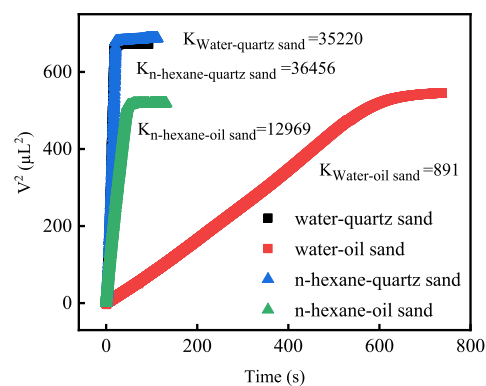
Figure 1. Wetting curves of quartz sand and oil sand in water and *n*-hexane.

hexane and water on quartz sand are close to each other, and the wetting slopes of *n*-hexane and water on oil sand show large differences. The LHR value of quartz sand was found to be 1.16 in the experimental results of Chang et al.,[19] which concluded that the surface wettability of quartz sand is relatively hydrophilic. In contrast, the LHR value of fruit shells was 66.87, which shows greater lipophilicity. Nikakhtari et al.[2] measured the water contact angle of oil sand by the fixed droplet method in the range of 80−88°. Liu et al.[24] determined the water contact angle of the oil sand by the Washburn method as 88.8 ± 0.9°, indicating that the oil sand is hydrophobic particles. And since the difference in polarity between oil sand and *n*-hexane is low, the wettability of *n*-hexane on oil sand is larger.[22] Therefore, the difference between the wetting slope of *n*-hexane and water on oil sand is large.

The wetting up process of droplets in capillaries can be analyzed according to Young's equation, which is mainly determined by air−liquid, solid−liquid, and air−solid inter-facial free energy. Hu et al.[36] found that in the system of air−water-quartz, quartz has high polarity with a surface free energy of about 76.0 mN/m, and the polarity of water is close to that of quartz.[27] In this paper, the measured contact angle of water droplets on the quartz sheet is 15.0°, and the surface tension of water is about 72.8 mN/m. The interfacial tension of quartz-water is about 5.7 mN/m, calculated according to Young's equation. Combining Young's equation and Washburn's capillary rise method, it is known that the air-quartz interfacial tension is the force that promotes the rise of the droplet in the capillary. The interfacial tension is greater than the sum of quartz-water interfacial tension and the vertical component of air−water interfacial tension. Therefore, the capillary force is conducive to the rise of droplets, and the slope of the wetting of quartz sand by water is greater. When the liquid phase is *n*-hexane, the air−liquid and solid−liquid interfacial tensions change. Due to the large difference in polarity between *n*-hexane and quartz, the interfacial tension of quartz-hexane becomes large. Meanwhile, the surface tension of *n*-hexane is about 18.3 mN/m, and the interfacial tension of air−liquid is greatly reduced compared with that of water. Hence the capillary combined force on the liquid droplet is still large, and the wetting slope of *n*-hexane on quartz sand is larger.

When the solid phase is oil sand and the liquid phase is water, the interfacial tension of air−solid of the system decreases and the interfacial tension of solid−liquid increases. At this time, the interfacial tension of air−oil sand is only

slightly greater than the component of surface tension of water and the interfacial tension of oil sand−water, and the capillary combined force is greatly reduced. Hence, the wetting slope of water on oil sand is lower. When the liquid phase is *n*-hexane, the interfacial tension of air−liquid and solid−liquid is reduced. And the interfacial tension of air−oil sand is greater than the fraction of surface tension of *n*-hexane and the interfacial tension of oil sand-*n*-hexane. Therefore, the capillary cohesion is conducive to the rise of liquid droplets, and the wetting slope of *n*-hexane and oil sand is larger.

3.2. Quartz Sand. For simplicity, similar primitive wetting curves are not provided. The $C \cdot \cos \theta$ values of quartz sand with different particle sizes in water, formamide, DMF, ethanol, cyclohexane, *n*-decane, and *n*-hexane are calculated by eq 4 and shown in Figure 2 as a function of surface tension of solvents.
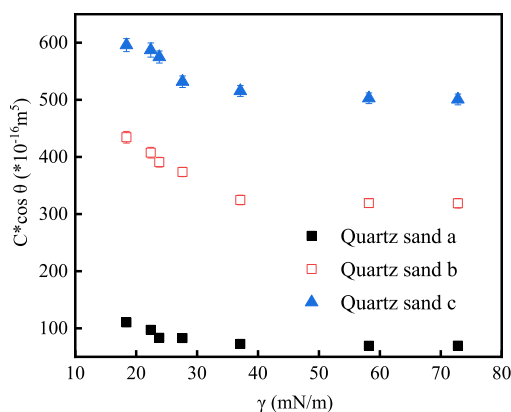
Figure 2. $C \cdot \cos \theta$ values of different solvents for quartz sand with different particle sizes.

The LHR value of quartz sand measured by Chang et al.[19] was 1.16. The LHR value is calculated by multiplying the slope of wetting of solid particles in cyclohexane and water (K) with the solvent viscosity (η) and dividing it by the surface tension of the solvent. The results in Figure 2 were substituted into the LHR equation to calculate the LHR values of quartz sand with different particle sizes. And it was found that the LHR of quartz sand a, quartz sand b, and quartz sand c was 1.10, 1.17, and 1.08, respectively, which was acceptable considering the measurement error. Therefore, the results obtained from the Washburn method measurements used in this paper are consistent with the qualitative results obtained in the literature.

For different particle sizes of quartz sand, the "geometry" of the powder bed is different, and the capillary constant C of quartz sand is different. According to eq 2, the capillary constant C is mainly affected by r, A, and ε, where A is the cross-sectional area of the sample tube, r is the effective pore radius of the powder bed, and ε is the void ratio of the powder material. Kirdponpattara et al.[37] found that the capillary constant C of the powder showed a gradual decrease with the gradual decrease of the powder particle size by studying the void size of powder with different particle sizes. Dang-Vu and Hupka[38] also found that larger particle sizes produced larger voids by studying solid particles of different particle sizes. Kong et al.[15] studied mineral powder of different particle sizes and found that the effective radius of the powder decreased with decreasing particle size of the mineral powder. Therefore, in the case of compact filling of the powder, the effective radius r of the powder bed, the void ratio ε of the powder material, and

the capillary constant C all gradually decrease when the particle size of the quartz sand gradually decreases.

The average value of the contact angle of water in the quartz sheet was measured to be 15.0° by the air−liquid−solid contact angle experiment. Then the capillary constants C for different grain sizes of quartz sand were calculated by substituting eq 1, and the capillary constants C of quartz sand are shown in Table 2 and Figure 3. It can be found that

Table 2. Capillary Constants C of Quartz Sand with Different Particle Sizes

powder samples	particle size (μm)	capillary constant C ($\times 10^{-16}$ m^5)	fitted slope
quartz sand a	177	8.15	
quartz sand b	147	6.41	
quartz sand c	125	5.18	$C = 0.052 \times d - 1.195$
quartz sand d	75	3.30	
quartz sand e	37	0.72	
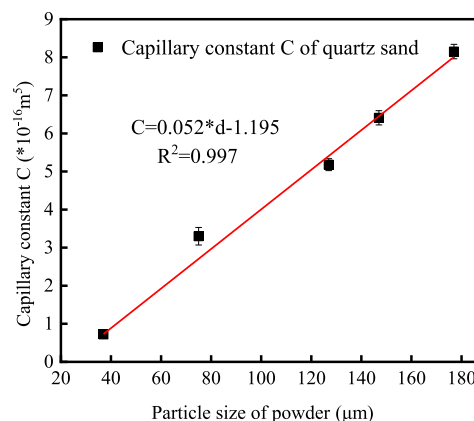
Figure 3. Fitting curve of the capillary constant C as a function of quartz sand size.

the calculation results are consistent with the above analysis, and the capillary constant C decreases with the decrease of quartz sand particle size. Meanwhile, the capillary constant C of quartz sand was linearly fitted, and the equation obtained from the fit is $C = 0.052 \times d - 1.195$.

As shown in Table 3, the powder contact angle of each solvent was calculated by substituting the above quartz sand capillary constant C into the value of $C \cdot \cos \theta$. It can be found that for the same particle size of quartz sand, the powder contact angle of the solvent is decreased with the decrease of the surface tension of the solvent. When the surface tension of the solvent is low enough, the powder contact angle of the solvent is 0°. Kong et al.[15] also found similar findings to the experimental results in Table 3, finding that for mineral particles of the same particle size, the contact angle decreases with decreasing surface tension of the solvent.

Van Oss et al.[39] determined the surface wettability of talc and illite in different solvents using the Washburn equation and thin-layer core absorption. The experimental results were found to be linear and shifted at a surface tension of 40 mN/m of the solvent. From Figure 2, it can be found that for the same particle size of quartz sand, the $C \cdot \cos \theta$ values show two linear

Table 3. Powder Contact Angles of Different Solvents on Quartz Sand with Different Particle Sizes[a]

contact angle (θ)	deionized water	formamide	DMF	cyclohexane	n-C$_{10}$	ethanol	n-C$_6$
quartz sand a	15.0 ± 0.3	14.1 ± 0.7	6.2 ± 0.2	0	0	0	0
quartz sand b	15.0 ± 0.3	14.7 ± 0.4	10.4 ± 0.8	0	0	0	0
quartz sand c	15.0 ± 0.3	15.4 ± 0.3	9.8 ± 0.4	0	0	0	0

[a]Here is the average value of the contact angle of water in the quartz sheet measured by the air−liquid−solid contact angle experiment.

relationships as the surface tension value of the solvent gradually increases. The first segment is when the surface tension is below 40 mN/m, and the $C \cdot \cos \theta$ value decreases rapidly with the increase of surface tension. Combined with the analysis in Figure 1, it can be seen that the increase of solid−liquid interfacial tension is lower than the decrease of the liquid surface tension when the polarity of the liquid decreases. Therefore, the contact angle values of the solvent on the quartz sand are all 0° for solvents with low polarity. The second segment is when the surface tension is higher than 40 mN/m, and the $C \cdot \cos \theta$ value decreases slowly with the increase of surface tension. At this stage, the increase in surface tension of the solvent is almost offset by the decrease in solid−liquid interfacial tension, and the $C \cdot \cos \theta$ value changes little.

Combining Young's equation and the OWRK method equation, eq 8 can be obtained, and the $\cos \theta$ value of the more suitable solvent is selected and substituted into eq 8. At the same time, according to the polar component γ_l^p and non-polar component γ_l^d of different solvents, the obtained γ_s^d and γ_s^p are added together, and the obtained γ_s is the surface free energy of quartz sand with different particle sizes, and the calculation results are shown in Table 4. The indicated free energies of

Table 4. Surface Free Energy of Quartz Sand with Different Particle Sizes

powder samples	particle size (μm)	surface free energy (mN/m)
quartz sand a	37	76.09
quartz sand b	75	76.65
quartz sand c	125	76.42

quartz sand a, quartz sand b, and quartz sand c calculated by the OWRK method are 76.09, 76.65, and 76.42 mN/m, respectively, which are close to the measured surface free energy of quartz of 76.00 mN/m in the literature.[36] Moreover, the particle size does not affect the calculation of surface free energy. Therefore, the experimental result shows that the method used in this paper can obtain the surface free energy of quartz sand.

3.3. Oil Sand. Figure 4 shows the $C \cdot \cos \theta$ values for oil sand of different particle sizes in different solvents. It was found that for the same solvent, the $C \cdot \cos \theta$ values of oil sand a, oil sand b, and oil sand c gradually decrease as their particle sizes decrease; this is similar to the results for different grain sizes of quartz sand in Figure 2. For oil sand with the same particle size, the $C \cdot \cos \theta$ value gradually decreases with the increasing surface tension of the solvent, and such a trend is similar to that of quartz sand. However, only a linear relationship was found for both oil sand a and oil sand b. This may be due to the larger voids between the particles of oil sand with larger particle size and the faster wetting rate of the solvent. When the particle size of the oil sand is small, the space between the particles is narrower. The time for the solvent to wet the oil sand is relatively longer, and the wetting rate is lower; hence, there are two fitted curves for oil sand c.
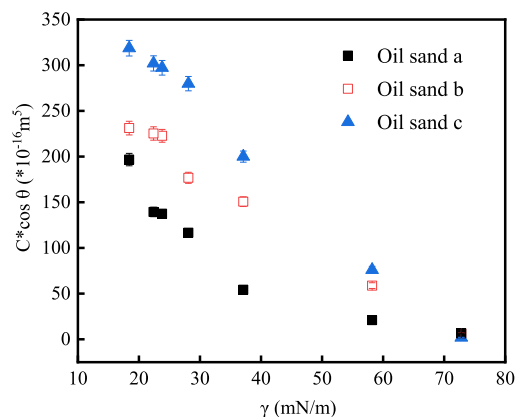
Figure 4. $C \cdot \cos \theta$ values of different solvents for oil sand with different particle sizes.

The particle size of oil sand is brought into the quartz sand capillary constant C fitting equation. Then the capillary constant C of oil sand with different particle sizes can be obtained, and the capillary constants C of oil sand a, oil sand b, and oil sand c are 11.81×10^{-16}, 8.01×10^{-16}, and 6.45×10^{-16} m^5, respectively. It can be found that with the gradual decrease of oil sand particle size, the capillary constant C of oil sand decreases subsequently.

Table 5 shows the powder contact angle of each solvent calculated by substituting the above oil sand capillary constant C into the value of $C \cdot \cos \theta$, and the water contact angle on the oil sand can be found to be around 89° by calculation. Liu et al.[24] determined the water contact angle of oil sand particles as 88.8 ± 0.9° according to the Washburn method, and Wang et al.[21] also obtained similar results by determining the water contact angle of oil sand (about 83−89°) by the WCR method. In addition, it can be seen from Table 5 that for the same particle size of oil sand particles, the powder contact angle of different solvents gradually decreases as the solvent surface tension decreases, which is similar to those of quartz particles.

According to the analysis results in Figure 1, it can be seen that for oil sand, when the solvent changes, both the interfacial tensions of air−liquid and solid−liquid in the system will change. When the solvents are water, formamide, and DMF, large difference in polarity between oil sand and solvents, the interfacial tension of solid−liquid is higher, and the contact angle of the solvent is larger. Therefore, the capillary force is lower at this time, the solvent wets the oil sand slowly, and the $C \cdot \cos \theta$ value is also lower. With the gradual decrease of solvent polarity, the interfacial tensions of air−liquid and solid−liquid of the system gradually decrease. As a result, this leads to both a decrease in the contact angle of the solvent and an increase in the capillary force, as well as an increase in the wetting rate of the oil sand and the value of $C \cdot \cos \theta$.

For the calculation of the surface free energy of the oil sand particles, the same method as above for calculating the surface free energy of quartz sand is used. The $\cos \theta$ value of the

Table 5. Powder Contact Angle of Different Solvents on Oil Sand with Different Particle Sizes

| contact angle (θ)	deionized water	formamide	DMF	cyclohexane	n-C$_{10}$	ethanol	n-C$_6$
oil sand a	88.8 ± 0.4	80.7 ± 0.9	74.2 ± 0.5	70.3 ± 0.6	69.2 ± 0.5	68.2 ± 0.6	65.3 ± 0.6
oil sand b	89.0 ± 0.5	77.5 ± 0.7	71.5 ± 0.4	67.1 ± 0.9	66.9 ± 0.5	65.1 ± 0.9	63.4 ± 0.7
oil sand c	89.7 ± 0.2	76.2 ± 0.3	69.7 ± 0.8	66.4 ± 0.6	64.2 ± 0.8	61.8 ± 0.4	60.4 ± 0.3

appropriate solvent is selected in Table 5 and substituted into eq 8. And then the calculated γ_l^p and γ_l^d are added together, the resulting γ_s is the surface free energy of oil sand of different particle sizes, and the calculation results are shown in Table 6.

Table 6. Surface Free Energy of Oil Sand with Different Particle Sizes

powder samples	particle size (μm)	surface free energy (mN/m)
oil sand a	147	23.22
oil sand b	177	23.45
oil sand c	250	23.63

The surface free energies of oil sand a, oil sand b, and oil sand c calculated by the OWRK method are 23.22, 23.45, and 23.63 mN/m, respectively. The calculated results are also reasonable for the hydrophobic oil sands.

3.4. Mineral Particles. Figure 5 shows the determination of the wettability of different mineral powder with different
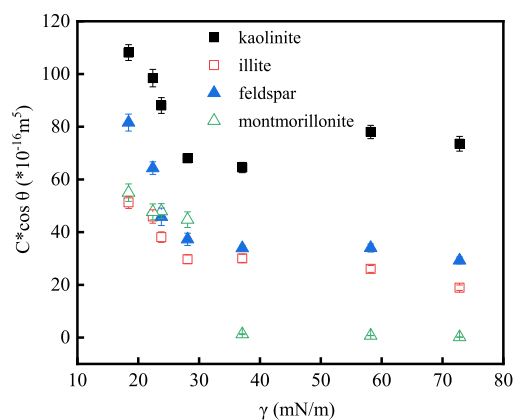
Figure 5. $C \cdot \cos \theta$ values of different solvents for different mineral particles.

solvents, and the $C \cdot \cos \theta$ values of different solvents were obtained by substituting the experimentally obtained data into eq 4. From Figure 5, it can be found that for the same mineral, the $C \cdot \cos \theta$ values of the minerals show two linear relationships as the surface tension of the solvent gradually increases. The first segment shows a rapid decrease in the $C \cdot \cos \theta$ values of the minerals when the surface tension value of the solvent is low. The second segment shows little change in the $C \cdot \cos \theta$ values when the surface tension of the solvent is greater than 40 mN/m. For the same solvent, the general pattern of $C \cdot \cos \theta$

values of different types of minerals: kaolinite > feldspar > illite > montmorillonite.

The particle sizes of the minerals are all about 44 μm, and then the particle size is brought into the quartz sand capillary constant C fitting equation, and the capillary constant C of different types of minerals can be obtained as 1.09×10^{-16} m^5.

The capillary constants C of different minerals are substituted into the $C \cdot \cos \theta$ values and the resulting contact angle values are shown in Table 7. It can be found that, for the same mineral, the contact angles of different solvents on minerals show a tendency to decrease with the gradual decrease of the solvent surface tension besides kaolinite. Kong et al.[15] also found that with a gradual decrease in the surface tension of the solvent, the contact angles of deionized water, formamide, and toluene with minerals gradually decrease. And for the same solvent, the contact angles of the minerals are kaolinite < feldspar < illite < montmorillonite in general.

Most minerals are of a certain polarity due to the presence of silica in the minerals.[37] For minerals with low polarity, when the polarity of the solvent is high, the interfacial tensions of the solid−liquid and the air−liquid are larger. Therefore, the contact angle is larger at this time.

On the other hand, it can be found from Table 7 that the water contact angle of kaolinite is lower compared to other minerals. This may be due to the higher polarity of kaolinite compared to other minerals and the lower solid−liquid interfacial tension of the system. Therefore, the contact angle of water on kaolinite is lower.

Substituting the appropriate $\cos \theta$ values from Table 7 into eq 8, the calculated surface free energies of kaolinite, illite, feldspar, and montmorillonite are 61.59, 32.85, 35.87, and 25.91 mN/m, respectively, as shown in Table 8. The mineral

Table 8. Surface Free Energy for Different Types of Mineral Particles

powder samples	particle size (μm)	surface free energy (mN/m)
kaolinite	44	61.59
illite	44	32.85
feldspar	44	35.87
MMT	44	25.91

particles with different polarity show the different value of surface free energy, and the kaolinite with the highest polarity has the highest value 61.59 mN/m, which can ensure the reliability of our method.

By the improved Washburn method in this paper, the surface free energy of a given solid particle can be calculated,

Table 7. Powder Contact Angles of Different Solvents on Different Types of Mineral Particles

contact angle (θ)	deionized water	formamide	DMF	cyclohexane	n-C$_{10}$	ethanol	n-C$_6$
kaolinite	47.2 ± 0.3	49.0 ± 0.8	58.1 ± 0.7	59.6 ± 0.8	44.4 ± 1.0	37.5 ± 0.5	30.1 ± 0.3
illite	77.0 ± 0.4	63.6 ± 0.3	62.1 ± 0.9	68.0 ± 0.4	62.2 ± 0.8	61.1 ± 0.7	61.5 ± 0.5
feldspar	73.1 ± 0.7	63.8 ± 0.4	58.6 ± 0.2	62.0 ± 0.7	57.7 ± 0.6	56.0 ± 0.9	48.5 ± 0.6
MMT	89.3 ± 0.9	88.2 ± 0.2	85.7 ± 0.3	69.4 ± 0.4	67.5 ± 0.4	62.8 ± 0.2	61.4 ± 0.4

which is very important in production practice and daily application.

4. CONCLUSIONS

In this work, the wettability of different solvents on the surface of powder with different hydrophilic/hydrophobic properties was determined by Washburn's capillary rise method, and the surface free energy of different powder was calculated by the OWRK method. The following conclusions can be obtained:

(1) It was found that the surface free energy and surface polarity of the powder gradually decrease as the hydrophilicity of the powder surface decreases. The solvents have strong wettability for all quartz with high surface free energy. For oil sands with low-energy surfaces, the wettability of solvents to oil sands gradually increases as the solvent surface tension decreases. In addition, the wettability of solvents for minerals is between that of quartz sand and oil sand.

(2) With the gradual decrease of the particle size of the powder, the capillary constant C of the powder gradually decreases. In addition, the surface free energy calculations for powders of different particle sizes exhibit the same results.

(3) The analysis by Young's equation and Washburn's capillary rise method shows that the capillary combined force on the droplet decreases with the gradual decrease of the surface free energy of the solid. Therefore, the infiltration rate of solvent gradually decreases, and the powder contact angle of solvent on the surface of solid particles gradually increases.

■ AUTHOR INFORMATION

Corresponding Authors

Feng Yan − *School of Chemistry, Tiangong University, Tianjin 300387, P. R. China;* ⊙ orcid.org/0000-0002-4855-5123; Email: yanfeng@tiangong.edu.cn

Lu Zhang − *Key Laboratory of Photochemical Conversion and Optoelectronic Materials, Technical Institute of Physics and Chemistry, Chinese Academy of Sciences, Beijing 100190, P. R. China;* ⊙ orcid.org/0000-0001-8355-900X; Email: luyiqiao@hotmail.com

Authors

Zheng Wang − *School of Chemistry, Tiangong University, Tianjin 300387, P. R. China*

Yanping Chu − *Exploration and Development Research Institute, Daqing Oil Field Company Limited, Daqing 163712, P. R. China*

Guozhong Zhao − *Exploration and Development Research Institute, Daqing Oil Field Company Limited, Daqing 163712, P. R. China; Heilongjiang Provincial Key Laboratory of Reservoir Physics & Fluid Mechanics in Porous Medium, Daqing 163712, P. R. China*

Zhilin Yin − *Exploration and Development Research Institute, Daqing Oil Field Company Limited, Daqing 163712, P. R. China; Heilongjiang Provincial Key Laboratory of Reservoir Physics & Fluid Mechanics in Porous Medium, Daqing 163712, P. R. China*

Tie Kuang − *Exploration and Development Research Institute, Daqing Oil Field Company Limited, Daqing 163712, P. R. China; Heilongjiang Provincial Key Laboratory of Reservoir*

Physics & Fluid Mechanics in Porous Medium, Daqing 163712, P. R. China

Lei Zhang − *Key Laboratory of Photochemical Conversion and Optoelectronic Materials, Technical Institute of Physics and Chemistry, Chinese Academy of Sciences, Beijing 100190, P. R. China*

Complete contact information is available at:
https://pubs.acs.org/10.1021/acsomega.3c01352

Notes

The authors declare no competing financial interest.

■ REFERENCES

(1) Zendehboudi, S.; Rezaei, N.; Chatzis, I. Effect of Wettability in Free-Fall and Controlled Gravity Drainage in Fractionally Wet Porous Media with Fractures. *Energy Fuels* **2011**, *25*, 4452−4468.

(2) Nikakhtari, H.; Wolf, S.; Choi, P.; Liu, Q.; Gray, M. R. Migration of Fine Solids into Product Bitumen from Solvent Extraction of Alberta Oilsands. *Energy Fuels* **2014**, *28*, 2925−2932.

(3) Alghunaim, A.; Kirdponpattara, S.; Newby, B.-m. Z. Techniques for determining contact angle and wettability of powders. *Powder Technol.* **2016**, *287*, 201−215.

(4) de Meijer, M.; Haemers, S.; Cobben, W.; Militz, H. Surface energy determinations of wood: Comparison of methods and wood species. *Langmuir* **2000**, *16*, 9352−9359.

(5) Buckton, G. Contact angle, adsorption and wettability—a review with respect to powders. *Powder Technol.* **1990**, *61*, 237−249.

(6) Dove, J. W.; Buckton, G.; Doherty, C. A comparison of two contact angle measurement methods and inverse gas chromatography to assess the surface energies of theophylline and caffeine. *Int. J. Pharm.* **1996**, *138*, 199−206.

(7) Shang, J.; Flury, M.; Harsh, J. B.; Zollars, R. L. Comparison of different methods to measure contact angles of soil colloids. *J. Colloid Interface Sci.* **2008**, *328*, 299−307.

(8) Susana, L.; Campaci, F.; Santomaso, A. C. Wettability of mineral and metallic powders: Applicability and limitations of sessile drop method and Washburn's technique. *Powder Technol.* **2012**, *226*, 68−77.

(9) Nowak, E.; Combes, G.; Stitt, E. H.; Pacek, A. W. A comparison of contact angle measurement techniques applied to highly porous catalyst supports. *Powder Technol.* **2013**, *233*, 52−64.

(10) Pan, C. C.; Feng, J. H.; Tian, Y. M.; Yu, L. P.; Luo, X. P.; Sheng, G. Y.; Fu, J. M. Interaction of oil components and clay minerals in reservoir sandstones. *Org. Geochem.* **2005**, *36*, 633−654.

(11) Rezaei Gomari, S.; Joseph, N. Study of the Effect of Clay Particles on Low Salinity Water Injection in Sandstone Reservoirs. *Energies* **2017**, *10*, 322.

(12) Robin, M.; Rosenberg, E.; Fassifihri, O. Wettability Studies at the Pore Level: A New Approach by Use of Cryo-SEM. *SPE Form. Eval.* **1995**, *10*, 11−19.

(13) Mamonov, A.; Aslanidis, P.; Fazilani, N.; Puntervold, T.; Strand, S. Influence of Sandstone Mineralogy on the Adsorption of Polar Crude Oil Components and Its Effect on Wettability. *Energy Fuels* **2022**, *36*, 10785−10793.

(14) Klimenko, A.; Molinier, V.; Bourrel, M. Mechanisms underlying the adhesion of crude oil to mineral surfaces: Relevance of oil-brine interactions. *J. Pet. Sci. Eng.* **2020**, *190*, 107036.

(15) Kong, L.; Mo, S.; Wang, N. High-Temperature Performance of Asphalt Mortar Using Surface and Interface Theory. *J. Mater. Civ. Eng.* **2015**, *27*, C4014009.

(16) Yan, F.; Qi, Y. H.; Fang, H. B.; Chen, D. L.; Liu, X. Y.; Jin, W. N. Synthesis and performances of branched hexadecanol polyethoxylene ester. *J. Tiangong Univ.* **2019**, *38*, 45−49.

(17) Fu, X. A.; Qutubuddin, S. Swelling behavior of organoclays in styrene and exfoliation in nanocomposites. *J. Colloid Interface Sci.* **2005**, *283*, 373−379.

(18) Yang, B. W.; Chang, Q. Wettability studies of filter media using capillary rise test. *Sep. Purif. Technol.* **2008**, *60*, 335−340.

(19) Chang, Q.; Wei, B.; He, Y. Capillary pressure method for measuring lipophilic hydrophilic ratio of filter media. *Chem. Eng. J.* **2009**, *150*, 323−327.

(20) Zhang, D.; Luo, R. An alternative method to evaluate the surface free energy of mineral fillers based on the generalized Washburn equation. *Constr. Build. Mater.* **2020**, *231*, 117164.

(21) Wang, C.; Geramian, M.; Liu, Q.; Ivey, D. G.; Etsell, T. H. Comparison of Different Methods To Determine the Surface Wettability of Fine Solids Isolated from Alberta Oil Sands. *Energy Fuels* **2015**, *29*, 3556−3565.

(22) Chen, F.; Finch, J. A.; Xu, Z.; Czarnecki, J. Wettability of fine solids extracted from bitumen froth. *J. Adhes. Sci. Technol.* **1999**, *13*, 1209−1224.

(23) Dang-Vu, T.; Jha, R.; Wu, S.-Y.; Tannant, D. D.; Masliyah, J.; Xu, Z. Wettability determination of solids isolated from oil sands. *Colloids Surf., A* **2009**, *337*, 80−90.

(24) Liu, J.; Wang, J.; Huang, J.; Cui, X.; Tan, X.; Liu, Q.; Zeng, H. Heterogeneous Distribution of Adsorbed Bitumen on Fine Solids from Solvent-Based Extraction of Oil Sands Probed by AFM. *Energy Fuels* **2017**, *31*, 8833−8842.

(25) Zelenev, A. S.; Grenoble, Z. Wettability of Reservoir Rocks Having Different Polarity by a Model Nonionic Surfactant: Fluid Imbibition Study into Crushed Rock Packs. *Energy Fuels* **2018**, *32*, 1340−1347.

(26) Zhu, Y.-q.; Yu, C.-x.; Li, Y.; Zhu, Q.-q.; Zhou, L.; Cao, C.; Yu, T.-t.; Du, F.-p. Research on the changes in wettability of rice (Oryza sativa.) leaf surfaces at different development stages using the OWRK method. *Pest Manage. Sci.* **2014**, *70*, 462−469.

(27) Zdziennicka, A.; Janczuk, B. Wettability of quartz in presence of nonionic surfactants and short chain alcohols mixtures. *J. Colloid Interface Sci.* **2010**, *343*, 594−601.

(28) Bilinski, B.; Holysz, L. Some theoretical and experimental limitations in the determination of surface free energy of siliceous solids. *Powder Technol.* **1999**, *102*, 120−126.

(29) Jaine, J. E.; Mucalo, M. R. Measurements of the wettability of catalyst support materials using the Washburn capillary rise technique. *Powder Technol.* **2015**, *276*, 123−128.

(30) Galet, L.; Patry, S.; Dodds, J. Determination of the wettability of powders by the Washburn capillary rise method with bed preparation by a centrifugal packing technique. *J. Colloid Interface Sci.* **2010**, *346*, 470−475.

(31) Buckton, G.; Newton, J. M. Assessment of the wettability of powders by use of compressed powder discs. *Powder Technol.* **1986**, *46*, 201−208.

(32) Katsanos, N. A.; Gavril, D.; Kapolos, J.; Karaiskakis, G. Surface energy of solid catalysts measured by inverse gas chromatography. *J. Colloid Interface Sci.* **2004**, *270*, 455−461.

(33) Fowkes, F. M. Determination of interfacial tensions, contact angles, and dispersion forces in surfaces by assuming additivity of intermolecular interactions in surfaces. *J. Phys. Chem.* **1962**, *66*, 382.

(34) Owens, D. K.; Wendt, R. Estimation of the surface free energy of polymers. *J. Appl. Polym. Sci.* **1969**, *13*, 1741−1747.

(35) Zhang, Q.; Zhou, Z.-H.; Hu, S.-S.; Li, S.-M.; Ma, D.-S.; Zhou, X.-Y.; Han, L.; Zhang, L.; Zhang, L. Wettability of a polymethylmethacrylate surface in the presence of benzyl-substituted alkyl betaines. *J. Mol. Liq.* **2019**, *277*, 571−576.

(36) Hu, B. Effect of Cationic and Zwitterionic Surfactants on Contact Angle of Quartz-Water-Crude Oil System. *J. Dispersion Sci. Technol.* **2016**, *37*, 1555−1562.

(37) Kirdponpattara, S.; Phisalaphong, M.; Newby, B.-M. Z. Applicability of Washburn capillary rise for determining contact angles of powders/porous materials. *J. Colloid Interface Sci.* **2013**, *397*, 169−176.

(38) Dang-Vu, T.; Hupka, J. Characterization of porous materials by capillary rise method. *Physicochem. Probl. Miner. Process.* **2005**, *39*, 47−65.

(39) Van Oss, C.; Giese, R.; Li, Z.; Murphy, K.; Norris, J.; Chaudhury, M.; Good, R. Determination of contact angles and pore sizes of porous media by column and thin layer wicking. *J. Adhes. Sci. Technol.* **1992**, *6*, 413−428.